
















Article

NGS-Based Molecular Karyotyping of Multiple Myeloma: Results from the GEM12 Clinical Trial

Juan Manuel Rosa-Rosa ^{1,2,*} , Isabel Cuenca ^{1,2} , Alejandro Medina ³, Iria Vázquez ⁴ , Andrea Sánchez-delaCruz ², Natalia Buenache ^{1,2}, Ricardo Sánchez ^{1,2} , Cristina Jiménez ^{3,5,6} , Laura Rosiñol ^{7,8} , Norma C. Gutiérrez ^{3,5,6} , Yanira Ruiz-Heredia ^{1,2,6} , Santiago Barrio ^{1,2,6}, Albert Oriol ⁹, María-Luisa Martín-Ramos ¹⁰, María-Jesús Blanchard ¹¹, Rosa Ayala ¹ , Rafael Ríos-Tamayo ¹², Anna Sureda ¹³, Miguel-Teodoro Hernández ¹⁴, Javier de la Rubia ¹⁵ , Gorka Alkorta-Aranburu ⁴, Xabier Agirre ^{4,6,16} , Joan Bladé ^{7,8}, María-Victoria Mateos ^{3,5,6} , Juan-José Lahuerta ⁶ , Jesús F. San-Miguel ^{4,6,16}, María-José Calasanz ⁴ , Ramón García-Sanz ^{3,5,6} , and Joaquín Martínez-Lopez ^{1,2,6,*}

- ¹ Hematology Department, Hospital 12 de Octubre, 28041 Madrid, Spain
 - ² H12O–CNIO Hematological Malignancies Clinical Research Unit, Spanish National Cancer Research (CNIO), 29029 Madrid, Spain
 - ³ Unidad de Biología Molecular-HLA, Laboratorio de Hematología, Hospital Universitario de Salamanca, 37007 Salamanca, Spain
 - ⁴ Center for Applied Medical Research (CIMA) LAB Diagnostics, Universidad de Navarra, 31008 Pamplona, Spain
 - ⁵ Cancer Research Institute of Salamanca-IBMCC (USAL-CSIC), 37007 Salamanca, Spain
 - ⁶ Centro de Investigación Biomédica en Red Cáncer (CIBERONC), 28029 Madrid, Spain
 - ⁷ Hospital Clinic de Barcelona, 08036 Barcelona, Spain
 - ⁸ August Pi i Sunyer Biomedical Research Institute (IDIBAPS), 08036 Barcelona, Spain
 - ⁹ Clinical Research Support Unit, Institut Català d'Oncologia, 08036 Barcelona, Spain
 - ¹⁰ Servicio de Genética, Hospital 12 de Octubre, 28041 Madrid, Spain
 - ¹¹ Hematology Department, Hospital Ramón y Cajal, 28034 Madrid, Spain
 - ¹² Hospital Universitario Puerta de Hierro, 28222 Majadahonda, Spain
 - ¹³ Institut Català d'Oncologia-I'Hospitalet, Institut de Investigació Biomèdica de Bellvitge (IDIBELL), Universitat de Barcelona, 08908 Barcelona, Spain
 - ¹⁴ Hospital Universitario de Canarias, 38320 Santa Cruz de Tenerife, Spain
 - ¹⁵ Hospital La Fe, 46026 Valencia, Spain
 - ¹⁶ Instituto de Investigaciones Sanitarias de Navarra (IdiSNA), Universidad de Navarra, 31008 Pamplona, Spain
- * Correspondence: juanm.rosa@gmail.com (J.M.-R.); jmarti01@ucm.es (J.M.-L.)



Citation: Rosa-Rosa, J.M.; Cuenca, I.; Medina, A.; Vázquez, I.; Sánchez-delaCruz, A.; Buenache, N.; Sánchez, R.; Jiménez, C.; Rosiñol, L.; Gutiérrez, N.C.; et al. NGS-Based Molecular Karyotyping of Multiple Myeloma: Results from the GEM12 Clinical Trial. *Cancers* **2022**, *14*, 5169. <https://doi.org/10.3390/cancers14205169>

Academic Editor: David Wong

Received: 16 September 2022

Accepted: 12 October 2022

Published: 21 October 2022

Publisher's Note: MDPI stays neutral with regard to jurisdictional claims in published maps and institutional affiliations.



Copyright: © 2022 by the authors. Licensee MDPI, Basel, Switzerland. This article is an open access article distributed under the terms and conditions of the Creative Commons Attribution (CC BY) license (<https://creativecommons.org/licenses/by/4.0/>).

Simple Summary: Multiple Myeloma (MM) is considered an incurable chronic disease, which prognosis depends on the presence of different genomic alterations. To accomplish a complete molecular diagnosis in a single assay, we have designed and validated a capture-based NGS approach to reliably identify pathogenic mutations (SNVs and indels), genomic alterations (CNVs and chromosomal translocations), and *IGH* rearrangements. We have observed a good correlation of the results obtained using our capture panel with data obtained by both FISH and WES techniques. In this study, the molecular classification performed using our approach was significantly associated with the stratification and outcome of MM patients. Additionally, this panel has been proven to detect specific *IGH* rearrangements that could be used as biomarkers in patient follow-ups through minimal residual disease (MRD) assays. In conclusion, we think that MM patients could benefit from the use of this capture-based NGS approach with a more accurate, single-assay molecular diagnosis.

Abstract: Next-generation sequencing (NGS) has greatly improved our ability to detect the genomic aberrations occurring in multiple myeloma (MM); however, its transfer to routine clinical labs and its validation in clinical trials remains to be established. We designed a capture-based NGS targeted panel to identify, in a single assay, known genetic alterations for the prognostic stratification of MM. The NGS panel was designed for the simultaneous study of single nucleotide and copy number variations, insertions and deletions, chromosomal translocations and V(D)J rearrangements. The panel was validated using a cohort of 149 MM patients enrolled in the GEM2012MENOS65 clinical trial. The results showed great global accuracy, with positive and negative predictive values close to 90% when

compared with available data from fluorescence in situ hybridization and whole-exome sequencing. While the treatments used in the clinical trial showed high efficacy, patients defined as high-risk by the panel had shorter progression-free survival ($p = 0.0015$). As expected, the mutational status of *TP53* was significant in predicting patient outcomes ($p = 0.021$). The NGS panel also efficiently detected clonal *IGH* rearrangements in 81% of patients. In conclusion, molecular karyotyping using a targeted NGS panel can identify relevant prognostic chromosomal abnormalities and translocations for the clinical management of MM patients.

Keywords: multiple myeloma; next generation sequencing; cytogenetics; high-risk

1. Introduction

Multiple myeloma (MM) is a heterogeneous disease with a complex clonal and sub-clonal architecture and with few recurrent mutations [1,2]. The expansion of genetic events, including translocations, copy number variations (CNVs) and point mutations, facilitates tumor progression and is also responsible for the short remissions and numerous relapses along the disease timeline [3]. Some of these genetic abnormalities have a major impact on prognosis [4].

However, only a few translocations and CNVs define outcome risk in patients with MM. Cytogenetic aberrations are routinely evaluated using fluorescence in situ hybridization (FISH) panels and single-nucleotide polymorphism (SNP) microarrays in bone marrow (BM)-isolated plasma cells of MM patients [4,5]. Deletion of 17p (del(17p)) and translocations t(4;14), t(4;16) and t(14;20) were identified as poor prognostic biomarkers; likewise, gain(1q) and del(1p) are considered high-risk features for some groups [3]. The coexistence of different chromosomal aberrations can also modify the prognostic risk—for example, trisomy of chromosome 3 or 5 is associated with a better prognosis in patients with tumors displaying other high-risk genetic features [6,7], whereas del(1p32) in patients with t(4;14), as well as del(6q) in patients with del(17p) and t(11;14) [8,9], increases the risk. In this context, the development of new molecular technologies has facilitated the classification of very high-risk patients who are characterized by either biallelic inactivation of *TP53* or amplification (≥ 4 copies) of 1q21 in patients presenting ISS-III (International Stage System) [10]. The presence of this “double-hit” high-risk signature is currently considered a key prognostic factor [10–12].

The advent of next-generation sequencing (NGS) has ushered in a new era of diagnostic understanding and classification of the genomic landscape of MM [3] and has revealed the presence of unique and shared mutations in coexisting subclones of malignant/pathogenic plasma cells (PPCs) and the absence of a universal driver mutation [2,3,13,14]. While several mutated genes have been described to date in MM, only loss-of-function mutations of *TP53* have had a clear prognostic impact. Accordingly, obtaining a complete genomic profile of MM, including single nucleotide variations (SNVs), insertion/deletion mutations (Indels), CNVs and translocations, would be crucial for the accurate diagnostic and prognostic stratification of MM patients. Along this line, there is great interest in the development of an NGS panel to identify—in a single assay—all possible chromosomal alterations (so-called molecular karyotype), which would considerably simplify the genomic diagnosis of patients with MM in a cost-effective manner [15–17] and would likely impact future targeted therapy approaches [18]. Although some efforts were made in this direction [15–17], the results have not been validated in cohorts of homogeneously treated patients with MM from clinical trials.

In the present study, we designed a capture-based targeted NGS panel to identify relevant genetic aberrations for the prognostic stratification of MM in a single assay. The panel aims to simultaneously detect SNVs, indels, CNVs, chromosomal translocations and V(D)J clonotypes [19] with a higher resolution and a smaller amount of required starting material than conventional techniques. NGS molecular karyotyping was validated and

compared with data from FISH and whole-exome sequencing (WES). We also clinically validated the MM-specific NGS panel in samples obtained at diagnosis from patients with MM enrolled in the GEM12 clinical trial [20]. Our findings suggest that this new approach could eventually replace the conventional and standard procedures used in laboratories for the molecular diagnosis of MM.

2. Materials and Methods

2.1. Patient Cohort and Samples

We studied genomic (g)DNA from CD138⁺ plasma cells of BM aspirates from 149 patients with newly diagnosed MM enrolled in the GEM2012MENOS65 clinical trial [21]. Patients with active newly diagnosed MM were treated according to the PETHEMA GEM2012MENOS65 and the companion PETHEMA/GEM2014MAIN clinical trials [21]. Each study site's independent ethics committee reviewed and approved the protocol, amendments, and informed consent forms. The study was designed and conducted per the ethical principles of the Declaration of Helsinki and the International Council for Harmonization Guidelines. The study was registered at www.clinicaltrials.gov (accessed on 27 September 2017) as #NCT01916252 and EudraCT as #2012-005683-10. To summarize, patients received VRd plus autologous stem cell transplantation, VRd consolidation and maintenance with Lenalidomide or Lenalidomide plus Ixazomib.

The clinicopathological features of the patients are summarized in Table 1. The average age at diagnosis was 60 years (range: 42–65), with a similar frequency for males (53%) and females (47%). The clinical characteristics of the patient cohort were representative of the patients included in the clinical trial [21]. Plasma cells from BM aspirates were enriched using anti-CD138⁺ immunomagnetic beads, obtaining a purity >85% in all cases. DNA was extracted using the AllPrep DNA/RNA Mini Kit (Qiagen, Hilden, Germany) and capture libraries were generated with the SureSelectQ^{XT} Reagent Kit (Agilent Technologies, Santa Clara, CA, USA) using 50 ng of genomic DNA. Libraries were multiplexed and sequenced on an Illumina NextSeq 500 platform (High Output Kit v2, Illumina, San Diego, CA, USA) in 150 bp paired-end mode.

Table 1. Main clinical patient characteristics. ECOG, Eastern Cooperative Oncology Group; ISS, International Staging System.

	Total in Our Study (N = 149) *	Total GEM2012MENOS65 Clinical Trial (N = 458) *
Median age (range) in years	60 (42–65)	58 (31–65)
Sex (%)		
Male	52.6	52.4
Female	47.4	47.6
ECOG performance status (%)		
0	47	42.6
1	35.6	39.7
2	15.2	13.5
3	2.3	3.5
Missing	2.3	0.7
M-protein type (%)		
IgG	63.7	59.6
IgA	20	23.4
Light chain	14.8	15.1
IgD	0	0.7
Nonsecretory	1.5	1.3

Table 1. Cont.

	Total in Our Study (N = 149) *	Total GEM2012MENOS65 Clinical Trial (N = 458) *
ISS stage (%)		
I	24.7	23.4
II	36	36.2
III	39.6	39.1
Missing	0	1.3
Lactate dehydrogenase elevated (%)		
Yes	8.1	14.2
No	77.8	82.1
Missing	14.1	3.7
High-risk cytogenetics (%)	19.7	20.1

* No significant differences were found between groups.

2.2. Capture Next-Generation Sequencing Panel Design

Two panel versions were used in this study; however, differences between panel versions are mainly focused on the improvement of coverage in the 14q32 region for translocation identification. Design was performed to detect the most common and relevant aberrations known to occur in MM [3], covering the coding regions of 26 genes involved in the development and progression of tumors (*ATM*, *ATR*, *ATRIP*, *BCL7A*, *BRAF*, *CCND1*, *CYLD*, *DIS3*, *EGR1*, *FAM46C*, *FGFR3*, *HIST1H1E*, *IRF4*, *KRAS*, *LTB*, *MAX*, *NRAS*, *NRM*, *PRDM1*, *PRKD2*, *RB1*, *TRAF3*, *ZFH4*, *CRBN* and *NFKB2*). Additionally, the complete exonic region was covered for *TP53*. Genes considered to be treatment targets or candidates for drug resistance in MM (*PSMD1*, *XBP1*, *PSMB5*, *PSMC2*, *PSMC6*, *DDB1*, *IKZF1* and *IKZF3*) [16–18] and genes related to new immunotherapy treatments (*CD38*, *CD19* and *SLAMF7*) were also included [22]. In addition, specific regions within canonical *IGH* locus (14q32) were included to capture *IGH* rearrangements, as well as germline polymorphisms distributed throughout the genome, to have a good representation of each chromosome to reliably detect CNVs. The total target size of the final design was 400 kb (SureDesign, <https://earray.chem.agilent.com/suredesign/index.htm> (accessed on 12 February 2019)). Design and order information are available upon request to corresponding authors.

2.3. Bioinformatic Analyses

Raw FASTQ files were evaluated using quality control checks from FastQC [23] and Trimmomatic [24] was used to remove low-quality bases, adapters and other technical sequencing artifacts. Each FASTQ file was aligned to the human reference genome (GRCh38/hg38) using Novoalign (<http://www.novocraft.com/products/novoalign/> (accessed on 1 March 2020)). Optical and PCR duplication elimination was carried out with Sambamba [25]. SNVs and indels were identified through the combination of VarScan2 [26] and bcftools [27]. Variants were annotated using several functional (RefSeq, Pfam), population-related (dbSNP, 1000 Genomes, ESP6500, ExAC, genomeAD), in silico functional impact prediction (dbNSFP, dbSNV), and cancer-related (COSMIC and ICGC) databases. Only variants described in the Catalog Of Somatic Mutations In Cancer database with prediction of the effect on protein function (codon stop, splicing, frameshift, non-synonymous and Indels) were selected and filtered considering the following parameters: *GMAF* population frequency ≤ 0.01 (obtained from any database), total coverage at position ≥ 50 , frequency of the variant in the sample ≥ 0.01 , absence of annotations indicative of an artifactual-type distribution/quality of reads, and distance to the design bed regions ≤ 200 . Potential CNVs were analyzed through an adaptation of the CONTRA v2.0.8 algorithm [28], using all samples as baseline. Breakpoint analysis was carried out with LUMPY [29] and Delly [30] to detect other potential rearrangements, selecting those events supported by more than 10 reads, followed by inspection of other rearrangement values (homology of consensus sequence, balance in the number of reads supporting each side of the breakpoint,

frequency of the breakpoint in the cohort, etc.). *IGH* rearrangements were evaluated using MiXCR [31] and Vidjil [31], ruling out those supported by <5 reads or presenting with a frequency <0.01.

2.4. Fluorescence In Situ Hybridization

The FISH panels for MM included probes to detect different translocations (t(4;14), t(6;14), t(11;14), t(14;16), t(14;20)) as well as alterations in chromosomal regions, such as chr1 (*CDKN2C/CKS1B*), chr8 (*MYC* BA), chr11 (*CCND1*), chr13 (*RB1/DLEU/LAMP*), chr14 (*IGH* BA), and chr17 (Iso(17p)), from MetaSystems Probes (AltLusheim, Germany). Only samples with clonality >15% were considered positive, with the exception of *TP53* (clonality >20%), as specified in the guidelines from the Spanish Myeloma Research Group (GEM) [32,33] to perform a better comparison against the whole clinical cohort.

2.5. Whole-Exome Sequencing

WES data were obtained from peripheral blood cells (control) and PPC (tumor) samples from 51 patients to validate the mutations, CNVs and translocations. Exome sequencing was performed using the SureSelect Human All Exon Kit (v5, 51 Mb, Agilent Technologies, Santa Clara, CA, USA) by MacroGen Inc. (Geumcheon-gu, Seoul, Korea), with an output of 0.6 Gb per sample. Bioinformatics analyses were performed as described above, except for total coverage at position that we used ≥ 10 instead of ≥ 50 . Those variants observed in control exome data were ruled out for consideration as germline variants. Loss of heterozygosity analysis was performed based on a selection of germline SNPs across the genome (minor allele frequency >0.3 and <0.7). Only CNVs observed on chromosomes 1 and 17 were reported.

2.6. Statistical Analyses

Statistical analyses were performed using RStudio and specific libraries from Bioconductor (<https://bioconductor.org/> (accessed on 25 May 2021)). Progression-free survival (PFS) was evaluated using Kaplan–Meier curves and two-sided log-rank tests. Multivariate analysis to determine hazard ratios was performed using the *coxph* and *ggforest* functions in R. The results were considered statistically significant at $p < 0.05$. Cytogenetic high-risk profile was considered if the selected CD138⁺ cells presented a translocation involving either chr4 or chr16 with chr14 (t(4;14)(p16;q32) and t(14;16)(q32;q23) or the presence of del(17p).

3. Results

3.1. Targeted Capture Next-Generation Sequencing Panel and Exome Statistics

Sequencing statistics were calculated for each panel version (see Supplementary Tables S1A and S2A). Panel 1 had an average of 7.3 million reads (range 3–14 million), which translated into a mean base depth of 1746 (range 567–3272) with an average fraction of bases of 88.5% (range 84–94%) at $>200\times$. The average reads in Panel 2 were 33 million for PPCs, resulting in a mean base depth of $2427\times$ (range 66–5967 \times) and 71% (range 8.58–88.85%) of bases at $>200\times$. Although the sequencing results were notably impacted by the quality of the sample DNA, the mean base depth was $>500\times$ for 91% (136 out of 149) of PPCs and the fraction of bases at $>200\times$ was $>75\%$ in 88% (131 out of 149) of cases from both panel versions. In addition, we estimated the mean base depth per million reads to be 239 (range 98–300) and 75 (range 2–165) for panel versions 1 and 2, respectively. Regarding the *IGH* genomic region, we observed an average of 1723 (range 709–3451) and 8691 (range 142–20,634) mapped reads in panels 1 and 2, respectively (see Supplementary Table S1B). Exome statistics are shown in Supplementary Tables S1C and S2. No significant differences were found between tumor and control sequencing data regarding the number of reads, coverage or depth distribution. The mean base depth was $66\times$ (range 63–116 \times) and $80\times$ (range 60–115 \times) for tumors and controls, respectively, indicating that no bias would be expected in SNV or CNV analyses.

3.2. Molecular Karyotyping Characterization of Patients with MM Using NGS Panels

The global molecular characterization of the 130 patients with at least one molecular alteration is shown in Figure 1. Below, we describe the different types of alterations, including SNVs, indels, CNVs, translocations and *IGH* rearrangements.

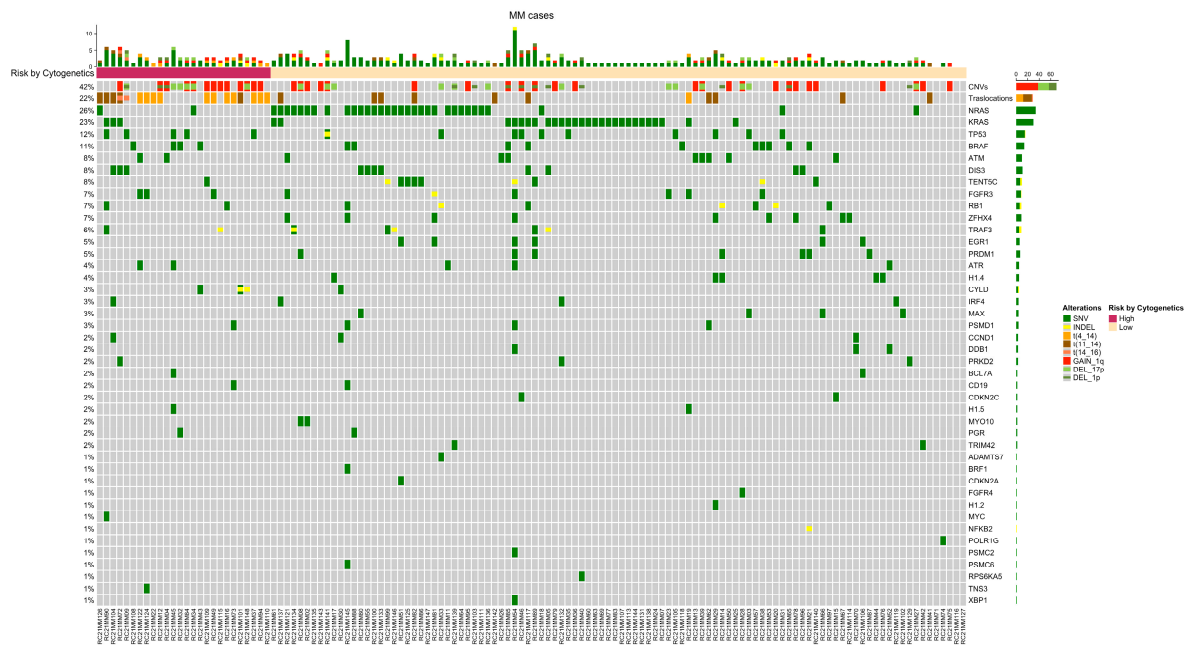


Figure 1. Molecular characterization. Patients were grouped based on the cytogenetic progression risk. CNVs and translocations are shown at the top. Alterations are represented in different colors.

SNVs and Indels: In total, 272 somatic mutations were found across 124 patients (see Supplementary Table S3), with an average of 1.7 (0–9) mutations per patient and at least one somatic mutation in approximately 82% of patients. Most of the mutations (253, 93%) were exonic and nonsynonymous SNVs, and 19 (7%) were short indels. As expected, the genes more frequently mutated in terms of percentage of patients carrying at least one mutation were *NRAS* (26%), *KRAS* (23%), *TP53* (12%), *BRAF* (11%), *DIS3* (8%), and *ATM* (8%).

Translocations and copy number variations: The NGS panel allows the identification of the three most frequent translocations described in MM, t(4;14), t(11;14) and t(14;16), and CNV identification was mainly focused on regions across chromosome arms 1p, 1q and 17q. Del(1p) was identified in 11 (7%) patients, whereas gain(1q) was observed in 39 (26%) patients (five patients showed both del(1p) and gain(1q)). Del(17p) was observed in eight (5%) patients. Regarding translocations, t(4;14) breakpoints were identified in 12 (8%) patients, t(11;14) breakpoints in 15 (10%) patients, and t(14;16) breakpoints in two (<2%) patients (Supplementary Table S4).

***IGH* VDJ rearrangements:** Overall, 185 functional *IGH* rearrangements were identified in 121 patients (81%) (Supplementary Tables S5 and S6). The number of rearrangements identified with MiXCR was larger than with Vidjil (165 vs. 117) and likewise was the number of patients (119 vs. 107) in which at least one rearrangement was identified. Rearrangements identified by MiXCR showed a higher average frequency (56% vs. 20%), but this could have been due to the final reads used to assemble the rearrangements (188 vs. 533 on average). A literature-based comparative study of major *IGH* clusters is presented in Supplementary Table S7 and Figure S1 shows a similar clonal detection rate between both techniques. In addition, *IGH* rearrangements observed in some of the patients were validated through PCR-based sequencing.

3.3. Comparative Results for NGS Panel, FISH and WES

Panel versus WES: Paired tumor-control WES data were available for 51 patients. Within the targeted regions, 47 somatic mutations were identified in the 51 patients using the NGS panel, and 37 of them (79%) were identified by WES (Supplementary Table S8). No somatic mutation was found in the WES data that was not present in the NGS panel data. The mean variant allele frequency (VAF) and depth for the NGS panel data were 0.23 (0.01–0.84) and $567\times$ ($134\text{--}920\times$), respectively, whereas the VAF and depth for the WES data were 0.26 (0.01–0.88) and $52\times$ ($9\text{--}182\times$), respectively. In the case of discordant positions (VAF = 0 in exome data), the mean VAF and depth were 0.04 (0.01–0.14) and 622 (166–891), respectively, for the NGS panel data, whereas in exome data, the average depth was 31 (10–50). The observed frequencies for del(1p), gain(1q) and del(17p) in the exome data were 10%, 29% and 4%, respectively, which were very similar to the frequencies obtained by the targeted approach (8%, 26% and 5%, respectively).

Panel versus FISH: Using FISH data as a reference, the NGS panel showed positive (PPV) and negative (NPV) predictive values of 0.90, with a sensitivity of 0.62, a specificity of 0.98 and a global accuracy of 0.90 (Table 2 (A)). For translocations only, PPV, NPV, sensitivity, specificity and global accuracy were 0.92, 0.93, 0.65, 0.99 and 0.92, respectively, and for CNVs were 0.89, 0.89, 0.61, 0.98 and 0.89, respectively. The combination of high-risk alterations (t(4;14), t(14;16), gain(1q), del(17p)) showed very similar concordant values (see Table 2 (A)). When compared to the CNV results from the WES data (Table 2 (B) and Table S9), PPV, NPV, sensitivity, specificity and global accuracy were 0.97, 0.96, 0.85, 0.99 and 0.96, respectively. Alteration-specific detailed PPV, NPV, sensitivity, specificity and global accuracy are shown in Table 2 and Table S10.

Table 2. Comparative estimators of our NGS panel against FISH and WES. (A) Estimated through comparison to FISH data. (B) Estimated through comparison to exome data. PPV = positive prognostic value, NPV = negative prognostic value. Tx = Translocations.

(A)	Alteration	PPV	NPV	Sensitivity	Specificity	Global Accuracy
	Tx + CNVs	0.90	0.90	0.62	0.98	0.90
	High-risk	0.88	0.91	0.65	0.98	0.91
	Tx	0.92	0.93	0.65	0.99	0.92
	t(4,14)	0.92	0.91	0.61	0.99	0.91
	t(11,14)	0.90	0.85	0.82	0.92	0.87
	t(14,16)	1.00	0.96	0.40	1.00	0.96
(B)	Alteration	PPV	NPV	Sensitivity	Specificity	Global Accuracy
	CNVs	0.97	0.96	0.85	0.99	0.96
	chr1p	1	0.93	0.73	1	0.94
	chr1q	1	0.94	0.88	1	0.96
	chr17	0.83	1	1	0.98	0.98

3.4. Impact of Molecular Karyotyping-Identified Alterations on Progression-Free Survival

Survival analyses were performed with data generated by the NGS-targeted panel (SNVs, CNVs and translocations) and with FISH data (CNVs and translocations). Regarding SNVs, only *TP53* mutational status had an impact on PFS ($p = 0.021$, Figure 2A), which was especially significant in cases presenting with homozygous (VAF > 0.5, mostly “double-hit”) mutations in *TP53* ($p < 0.0001$). The impact on PFS of the different structural genomic alterations (t(4;14), t(11;14), t(14;16), del(1p), gain(1q), del(17p)) revealed that only gain(1q) from NGS data was significant (NGS $p = 0.027$ vs. FISH $p = 0.2$, Figure 2A). The impact of del(17p) alone was not significant for PFS independent of the technique ($p > 0.5$, Figure 2A). Using NGS data, we defined a high-risk profile based on classical genetic high-risk alterations (del(17p), gain(1q) and translocations t(4;14)/t(14;16)) adding the mutational status of *TP53*, which significantly predicted ($p = 0.0015$, Figure 2A) the outcome of this cohort of patients. Multivariable analysis (Figure 2B) confirmed the significant impact of the high-risk profile ($p = 0.015$) and of homozygous mutations in *TP53*

($p = 0.002$), multiplying the progression hazard risk by 2.34 (CI = 1.18–4.7, $p = 0.015$) and 6.35 (CI = 1.94–20.9, $p = 0.002$) times, respectively.

(A)

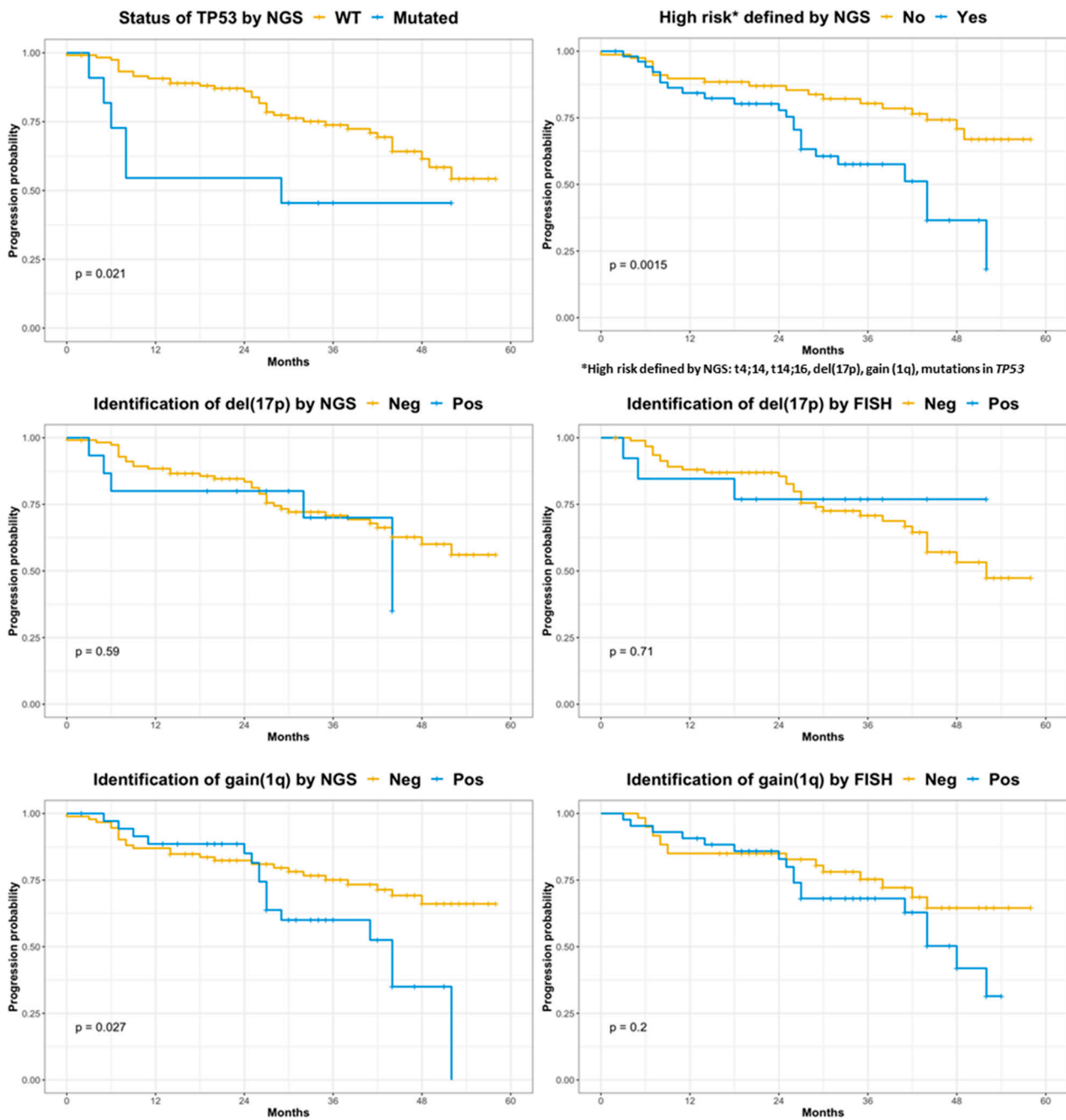


Figure 2. Cont.

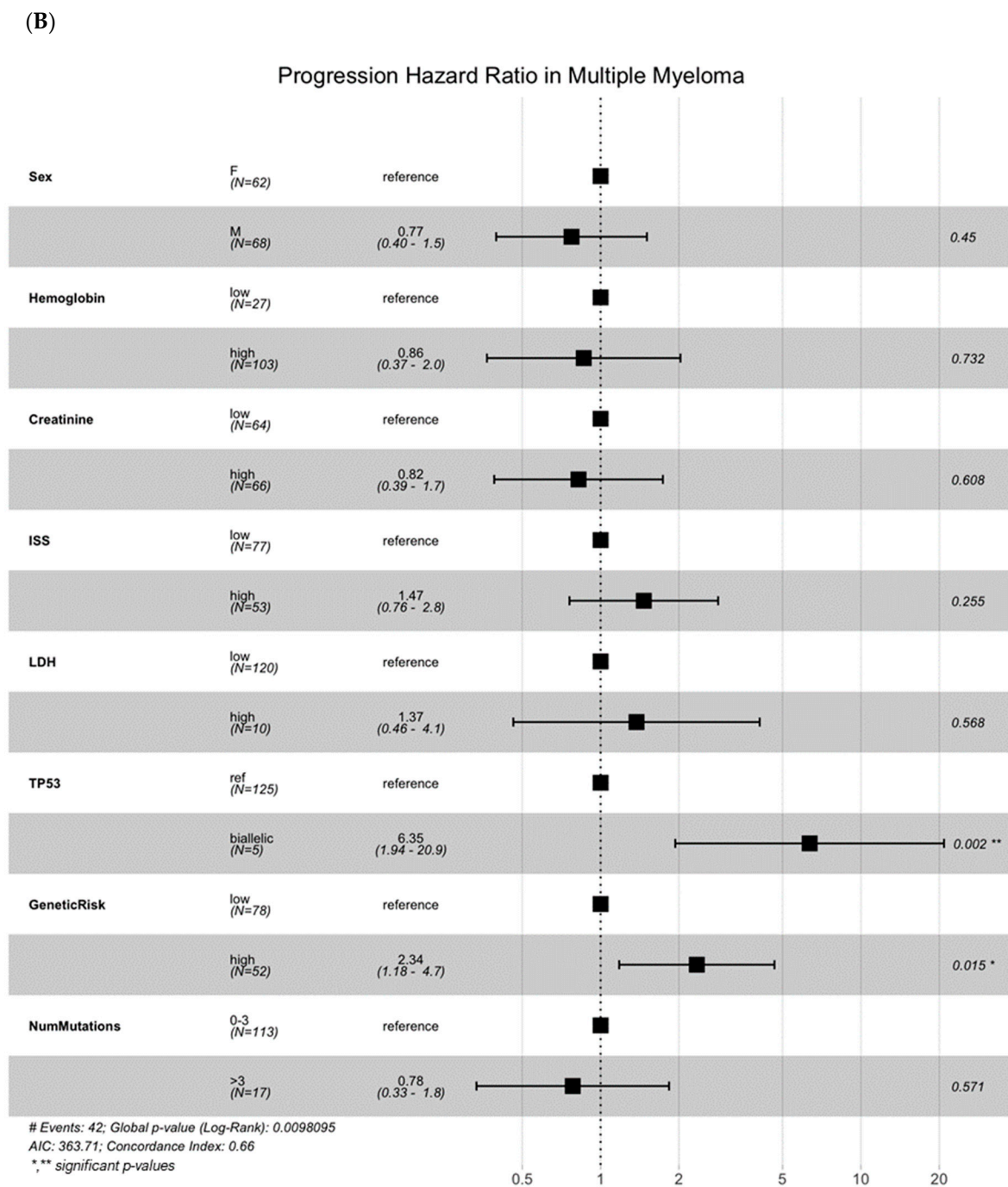


Figure 2. Impact of specific alterations on the progression of MM. (A) Univariate survival analysis (Kaplan–Meier plots). *TP53* mutations and high-risk by NGS plots are shown at the top; del(17p) identified by NGS or FISH plots are shown in the middle; and gain(1q) identified by NGS or FISH plots are shown at the bottom. (B) Multivariable analysis using *coxph* and *ggforest* functions. Selected values were sex, hemoglobin (high > 9 g/dL), creatinine (high > 1 mg/dL), International Staging System stage (high = ISS III), LDH (lactate dehydrogenase, high = abnormal), *TP53* mutational status, genetic high-risk, and total number of mutations.

4. Conclusions

We show here that our targeted NGS panel based on molecular karyotyping can detect, in a single assay and with high precision, the key genomic alterations for MM stratification, including CNVs, SNVs, *IGH* clonal rearrangements and translocations. Moreover, the identification of an MM high-risk genetic profile with the NGS panel showed a suitable cor-

relation with current gold standard techniques: FISH for CNVs and translocations and WES for CNVs and SNVs. Other targeted sequencing panels were previously reported [15,16,34] but with limitations in all cases, such as the inability to detect either translocations, CNVs or *IGH* rearrangements.

The genes often affected in MM are deeply covered by our panel, allowing the detection of both SNVs and indels at a similar frequency to that described in the literature. As expected, the comparative analysis with WES data revealed a greater sensitivity in coding regions targeted by our panel. WES-limited depth across targeted genes could have hampered the detection of mutations, with a VAF of 1–5% [2,35]. According to our results, current standard WES parameters and mean base depth would make it an unreliable tool for the identification of mutations within relevant genes in MM.

The sensitivity shown for translocations reached an average of 60% when compared to FISH data. In this regard, the small number of positive cases (23%) might have negatively affected estimates of the sensitivity to detect translocations. Published results are similar [15,34], pointing out the difficulty in detecting translocations by NGS. Since the nature of the genomic regions prone to produce translocation breakpoint is complex (masked, repetitive homologous regions), the efficiency of the whole process depends on random facts such as where DNA breakpoints occur during the fragmentation step or the efficiency of the probes specific of these regions.

Moreover, we observed no bias in the identification of different events, although *del(1p)* and *t(14;16)* presented a lower sensitivity. Taking into account the results obtained from CNVs using WES data, we concluded that this low sensitivity is probably due to FISH limitations in the case of *del(1p)*, derived from the location of the probe; and panel limitations in the case of *t(14;16)*. We are currently working on different improvements in the design of the NGS panel that could increase the sensitivity to detect some of the translocations and CNVs.

On the other hand, we found excellent global accuracy, PPV and NPV (approximately 90%) for the NGS panel when the results were compared with available FISH data. Given that FISH analysis has a limit of detection of approximately 10%, and that FISH is only able to show the presence of a maximum of two concomitant alterations in the same cell clone, we consider that our NGS panel can be a valid diagnostic tool.

The NGS panel was superior to FISH for CNV detection, which was confirmed by WES data. This is likely because FISH probes are designed in very specific locations within chromosomes and partial deletions/gains can occur in more telomeric/centromeric regions that do not affect the FISH signal. An example of this is shown in Supplementary Figure S2 (left), in which partial deletions/gains were identified by WES and the NGS panel but not by FISH. Additionally, as shown in Supplementary Figure S2 (right), alterations spreading a shorter length could be identified more precisely with either FISH or NGS panel data that go beyond the resolution of WES. The importance of these specific cases is shown by the difference observed in the impact on PFS. In our cohort of patients, the impact of gain (1q) was significant ($p = 0.027$) using panel data (see Figure 2A) and not when using FISH.

Disease progression is a key event in MM and the stratification of high-risk profiles remains an important goal to guide clinical decision-making [5]. Our results show that the accuracy of the NGS panel for the identification of high-risk patients with short PFS is superior to that of the other genetic techniques. Notably, our approach was able to identify patients with poor outcomes even though this series of patients received highly effective treatments [21].

The main limitation was the small number of true positive cases for some specific alterations, leading to a smaller sensitivity than recent studies [36]. Increasing the density of probes in certain regions for CNV and breakpoint detection is the next step. In return, a strength of our study is the fact that all the patients were homogeneously treated in a clinical trial.

In conclusion, molecular karyotyping by our targeted captured-based NGS panel specific for MM identifies SNVs, CNVs, *IGH* clonal rearrangements and translocations

relevant to MM management. Although this approach has the potential to replace conventional cytogenetic approaches for the definition of genomic high-risk genomic profiles, simplifying the genetic study of MM, improvements in panel design will be addressed to improve the sensitivity to detect translocation events.

Supplementary Materials: The following supporting information can be downloaded at: <https://www.mdpi.com/article/10.3390/cancers14205169/s1>, Figure S1: Distribution of major IGH gene clusters involved in the rearrangements identified in 5 different studies [37–40]; Figure S2: Visual representation of CNV data in chromosomes 1 and 17 from two different patients; Table S1: Sequencing statistics; Table S2: Raw sequencing statistics for each sample. (A) Panel data. (B) WES data; Table S3: SNVs and indels identified in MM patients; Table S4: Comparative table between FISH and NGS results, related to FISH probe locations; Table S5: IGH arrangement summary of PPCs; Table S6: IG rearrangements identified by using both MiXCR and Vidjil; Table S7: IG rearrangement identification comparative study; Table S8: Comparative mutational results from exome and panel data; Table S9: CNV events identified by panel and exome analysis across chromosomes 1 and 17; Table S10: Estimation of PPV, NPV, sensitivity, specificity and global accuracy.

Author Contributions: Conceptualization, J.B., M.-V.M., J.-J.L., J.F.S.-M., M.-J.C., R.G.-S. and J.M.-L.; Data curation, J.M.R.-R. and I.C.; Formal analysis, J.M.R.-R., I.C., A.S.-d. and N.B.; Funding acquisition, J.M.-L.; Investigation, N.C.G., M.-L.M.-R., M.-J.B., R.A., R.R.-T., A.S., M.-T.H., J.d.I.R., G.A.-A., J.F.S.-M. and J.M.-L.; Methodology, J.M.R.-R., A.M., I.V., R.S., L.R., Y.R.-H., S.B., A.O. and X.A.; Resources, J.M.-L.; Supervision, C.J., L.R. and N.C.G.; Writing—original draft, J.M.R.-R.; Writing—review & editing, J.F.S.-M., M.-J.C., R.G.-S. and J.M.-L. All authors have read and agreed to the published version of the manuscript.

Funding: The study was supported by the Accelerator Grant: next steps: Early detection and intervention: Understanding the mechanisms of transformation and hidden resistance of incurable hematological malignancies, grants from Instituto de Salud Carlos III PI15/01484 and CRIS Foundation 2020/0063 and 2021/0088.

Institutional Review Board Statement: The study was conducted in accordance with the Declaration of Helsinki, and approved by the Ethics Committee of Instituto de Investigación Hospital 12 de Octubre (i+12)-FIBH12O, project associated code 15/01484, 14 of July 2015.

Informed Consent Statement: Informed consent was obtained from all subjects involved in the study.

Data Availability Statement: The data not presented in this article can be shared up on request.

Acknowledgments: We would like to thank David Gómez-Sánchez from Lung Cancer Unit (Hospital 12 Octubre), for his support and advices in the first steps of this project.

Conflicts of Interest: The authors declare no conflict of interest.

References

1. Borello, I. Can We Change the Disease Biology of Multiple Myeloma? *Leuk. Res.* **2012**, *36* (Suppl. 1), S3–S12. [[CrossRef](#)]
2. Bolli, N.; Avet-Loiseau, H.; Wedge, D.C.; van Loo, P.; Alexandrov, L.B.; Martincorena, I.; Dawson, K.J.; Iorio, F.; Nik-Zainal, S.; Bignell, G.R.; et al. Heterogeneity of Genomic Evolution and Mutational Profiles in Multiple Myeloma. *Nat. Commun.* **2014**, *5*, 2997. [[CrossRef](#)] [[PubMed](#)]
3. Walker, B.A.; Boyle, E.M.; Wardell, C.P.; Murison, A.; Begum, D.B.; Dahir, N.B.; Proszek, P.Z.; Johnson, D.C.; Kaiser, M.F.; Melchor, L.; et al. Mutational Spectrum, Copy Number Changes, and Outcome: Results of a Sequencing Study of Patients with Newly Diagnosed Myeloma. *J. Clin. Oncol.* **2015**, *33*, 3911. [[CrossRef](#)] [[PubMed](#)]
4. Manier, S.; Salem, K.Z.; Park, J.; Landau, D.A.; Getz, G.; Ghobrial, I.M. Genomic Complexity of Multiple Myeloma and Its Clinical Implications. *Nat. Rev. Clin. Oncol.* **2017**, *14*, 100–113. [[CrossRef](#)]
5. Sonneveld, P.; Avet-Loiseau, H.; Lonial, S.; Usmani, S.; Siegel, D.; Anderson, K.C.; Chng, W.J.; Moreau, P.; Attal, M.; Kyle, R.A.; et al. Treatment of Multiple Myeloma with High-Risk Cytogenetics: A Consensus of the International Myeloma Working Group. *Blood* **2016**, *127*, 2955–2962. [[CrossRef](#)]
6. Avet-Loiseau, H.; Hulin, C.; Campion, L.; Rodon, P.; Marit, G.; Attal, M.; Royer, B.; Dib, M.; Voillat, L.; Bouscary, D.; et al. Chromosomal Abnormalities Are Major Prognostic Factors in Elderly Patients with Multiple Myeloma: The Intergroupe Francophone Du Myélome Experience. *J. Clin. Oncol.* **2013**, *31*, 2806–2809. [[CrossRef](#)]

7. Kumar, S.; Fonseca, R.; Ketterling, R.P.; Dispenzieri, A.; Lacy, M.Q.; Gertz, M.A.; Hayman, S.R.; Buadi, F.K.; Dingli, D.; Knudson, R.A.; et al. Trisomies in Multiple Myeloma: Impact on Survival in Patients with High-Risk Cytogenetics. *Blood* **2012**, *119*, 2100–2105. [[CrossRef](#)]
8. Hebraud, B.; Magrangeas, F.; Cleyne, A.; Lauwers-Cances, V.; Chretien, M.L.; Hulin, C.; Leleu, X.; Yon, E.; Marit, G.; Karlin, L.; et al. Role of Additional Chromosomal Changes in the Prognostic Value of t(4;14) and Del(17p) in Multiple Myeloma: The IFM Experience. *Blood* **2015**, *125*, 2095–2100. [[CrossRef](#)]
9. Leiba, M.; Duek, A.; Amariglio, N.; Avigdor, A.; Benyamini, N.; Hardan, I.; Zilbershats, I.; Ganzel, C.; Shevetz, O.; Novikov, I.; et al. Translocation t(11;14) in Newly Diagnosed Patients with Multiple Myeloma: Is It Always Favorable? *Genes Chromosomes Cancer* **2016**, *55*, 710–718. [[CrossRef](#)]
10. Walker, B.A.; Mavrommatis, K.; Wardell, C.P.; Ashby, T.C.; Bauer, M.; Davies, F.; Rosenthal, A.; Wang, H.; Qu, P.; Hoering, A.; et al. A High-Risk, Double-Hit, Group of Newly Diagnosed Myeloma Identified by Genomic Analysis. *Leukemia* **2019**, *33*, 159–170. [[CrossRef](#)]
11. Rajkumar, S.V. Multiple Myeloma: 2020 Update on Diagnosis, Risk-Stratification and Management. *Am. J. Hematol.* **2020**, *95*, 548–567. [[CrossRef](#)]
12. Liu, X.L.; Yang, Y.P.; Bai, J.; Yue, T.T.; Yang, P.Y.; Zhang, Y.; Fan, H.Q.; Li, W.; Jin, F.Y. Adverse Effects of Double-Hit Combining ISS-III Stage and 1q Gain or Del (17p) on Prognosis of Patients with Newly Diagnosed Multiple Myeloma. *Zhonghua Xue Ye Xue Za Zhi* **2019**, *40*, 912–917. [[CrossRef](#)] [[PubMed](#)]
13. Morgan, G.J.; Walker, B.A.; Davies, F.E. The Genetic Architecture of Multiple Myeloma. *Nat. Rev. Cancer* **2012**, *12*, 335–348. [[CrossRef](#)] [[PubMed](#)]
14. JLoehr, J.G.; Stojanov, P.; Carter, S.L.; Cruz-Gordillo, P.; Lawrence, M.S.; Auclair, D.; Sougnez, C.; Knoechel, B.; Gould, J.; Saksena, G.; et al. Widespread Genetic Heterogeneity in Multiple Myeloma: Implications for Targeted Therapy. *Cancer Cell* **2014**, *25*, 91–101. [[CrossRef](#)]
15. Yellapantula, V.; Hultcrantz, M.; Rustad, E.H.; Wasserman, E.; Londono, D.; Cimera, R.; Ciardiello, A.; Landau, H.; Akhlaghi, T.; Mailankody, S.; et al. Comprehensive Detection of Recurring Genomic Abnormalities: A Targeted Sequencing Approach for Multiple Myeloma. *Blood Cancer J.* **2019**, *9*, 101. [[CrossRef](#)]
16. Ruiz-Heredia, Y.; Sánchez-Vega, B.; Onecha, E.; Barrio, S.; Alonso, R.; Martínez-ávila, J.C.; Cuenca, I.; Agirre, X.; Braggio, E.; Hernández, M.T.; et al. Mutational Screening of Newly Diagnosed Multiple Myeloma Patients by Deep Targeted Sequencing. *Haematologica* **2018**, *103*, e544–e548. [[CrossRef](#)]
17. Kortuem, K.M.; Braggio, E.; Bruins, L.; Barrio, S.; Shi, C.S.; Zhu, Y.X.; Tibes, R.; Viswanatha, D.; Votruba, P.; Ahmann, G.; et al. Panel Sequencing for Clinically Oriented Variant Screening and Copy Number Detection in 142 Untreated Multiple Myeloma Patients. *Blood Cancer J.* **2016**, *6*, 351–355. [[CrossRef](#)]
18. Sacco, A.; Federico, C.; Todoerti, K.; Ziccheddu, B.; Palermo, V.; Giacomini, A.; Ravelli, C.; Maccarinelli, F.; Bianchi, G.; Belotti, A.; et al. Specific Targeting of the KRAS Mutational Landscape in Myeloma as a Tool to Unveil the Elicited Antitumor Activity. *Blood* **2021**, *138*, 1705–1720. [[CrossRef](#)]
19. Martínez-López, J.; Sanchez-Vega, B.; Barrio, S.; Cuenca, I.; Ruiz-Heredia, Y.; Alonso, R.; Rapado, I.; Marin, C.; Cedena, M.T.; Paiva, B.; et al. Analytical and Clinical Validation of a Novel In-House Deep-Sequencing Method for Minimal Residual Disease Monitoring in a Phase II Trial for Multiple Myeloma. *Leukemia* **2017**, *31*, 1446–1449. [[CrossRef](#)]
20. Rosiñol, L.; Oriol, A.; Rios, R.; Sureda, A.; Blanchard, M.J.; Hernández, M.T.; Martínez-Martínez, R.; Moraleda, J.M.; Jarque, I.; Bargay, J.; et al. Bortezomib, Lenalidomide, and Dexamethasone as Induction Therapy Prior to Autologous Transplant in Multiple Myeloma. *Blood* **2019**, *134*, 1337–1345. [[CrossRef](#)]
21. Jiménez-Ubieto, A.; Paiva, B.; Puig, N.; Cedena, M.T.; Martínez-López, J.; Oriol, A.; Blanchard, M.J.; Ríos, R.; Martín, J.; Martínez, R.; et al. Validation of the International Myeloma Working Group Standard Response Criteria in the PETHEMA/GEM2012MENOS65 Study: Are These Times of Change? *Blood* **2021**, *138*, 1901–1905. [[CrossRef](#)] [[PubMed](#)]
22. Misiewicz-Krzeminska, I.; de Ramón, C.; Corchete, L.A.; Krzeminski, P.; Rojas, E.A.; Isidro, I.; García-Sanz, R.; Martínez-López, J.; Oriol, A.; Bladé, J.; et al. Quantitative Expression of Ikaros, IRF4, and PSMD10 Proteins Predicts Survival in VRD-Treated Patients with Multiple Myeloma. *Blood Adv.* **2020**, *4*, 6023–6033. [[CrossRef](#)] [[PubMed](#)]
23. Andrews, S. *FastQC: A Quality Control Tool for High Throughput Sequence Data*; Babraham Bioinformatics: Cambridge, UK, 2010.
24. Bolger, A.M.; Lohse, M.; Usadel, B. Trimmomatic: A Flexible Trimmer for Illumina Sequence Data. *Bioinformatics* **2014**, *30*, 2114. [[CrossRef](#)] [[PubMed](#)]
25. Tarasov, A.; Vilella, A.J.; Cuppen, E.; Nijman, I.J.; Prins, P. Sambamba: Fast Processing of NGS Alignment Formats. *Bioinformatics* **2015**, *31*, 2032–2034. [[CrossRef](#)]
26. Koboldt, D.C.; Zhang, Q.; Larson, D.E.; Shen, D.; McLellan, M.D.; Lin, L.; Miller, C.A.; Mardis, E.R.; Ding, L.; Wilson, R.K. VarScan 2: Somatic Mutation and Copy Number Alteration Discovery in Cancer by Exome Sequencing. *Genome Res.* **2012**, *22*, 568–576. [[CrossRef](#)]
27. Danecek, P.; Bonfield, J.K.; Liddle, J.; Marshall, J.; Ohan, V.; Pollard, M.O.; Whitwham, A.; Keane, T.; McCarthy, S.A.; Davies, R.M.; et al. Twelve Years of SAMtools and BCFtools. *Gigascience* **2021**, *10*, giab008. [[CrossRef](#)] [[PubMed](#)]
28. Li, J.; Lupat, R.; Amarasinghe, K.C.; Thompson, E.R.; Doyle, M.A.; Ryland, G.L.; Tothill, R.W.; Halgamuge, S.K.; Campbell, I.G.; Gorrington, K.L. CONTRA: Copy Number Analysis for Targeted Resequencing. *Bioinformatics* **2012**, *28*, 1307. [[CrossRef](#)]

29. Layer, R.M.; Chiang, C.; Quinlan, A.R.; Hall, I.M. LUMPY: A Probabilistic Framework for Structural Variant Discovery. *Genome Biol.* **2014**, *15*, R84. [[CrossRef](#)]
30. Rausch, T.; Zichner, T.; Schlattl, A.; Stütz, A.M.; Benes, V.; Korbel, J.O. DELLY: Structural Variant Discovery by Integrated Paired-End and Split-Read Analysis. *Bioinformatics* **2012**, *28*, i333. [[CrossRef](#)]
31. Duez, M.; Giraud, M.; Herbert, R.; Rocher, T.; Salson, M.; Thonier, F. Vidjil: A Web Platform for Analysis of High-Throughput Repertoire Sequencing. *PLoS ONE* **2016**, *11*, e0166126. [[CrossRef](#)]
32. Paiva, B.; Gutiérrez, N.C.; Rosiñol, L.; Vidriales, M.B.; Montalbán, M.Á.; Martínez-López, J.; Mateos, M.V.; Cibeira, M.T.; Cordón, L.; Oriol, A.; et al. High-Risk Cytogenetics and Persistent Minimal Residual Disease by Multiparameter Flow Cytometry Predict Unsustained Complete Response after Autologous Stem Cell Transplantation in Multiple Myeloma. *Blood* **2012**, *119*, 687–691. [[CrossRef](#)] [[PubMed](#)]
33. Thakurta, A.; Ortiz, M.; Blecua, P.; Towfic, F.; Corre, J.; Serbina, N.V.; Flynt, E.; Yu, Z.; Yang, Z.; Palumbo, A.; et al. High Subclonal Fraction of 17p Deletion Is Associated with Poor Prognosis in Multiple Myeloma. *Blood* **2019**, *133*, 1217–1221. [[CrossRef](#)] [[PubMed](#)]
34. Jiménez, C.; Jara-Acevedo, M.; Corchete, L.A.; Castillo, D.; Ordóñez, G.R.; Sarasquete, M.E.; Puig, N.; Martínez-López, J.; Prieto-Conde, M.I.; García-Álvarez, M.; et al. A Next-Generation Sequencing Strategy for Evaluating the Most Common Genetic Abnormalities in Multiple Myeloma. *J. Mol. Diagn.* **2017**, *19*, 99–106. [[CrossRef](#)] [[PubMed](#)]
35. Walker, B.A.; Mavrommatis, K.; Wardell, C.P.; Cody Ashby, T.; Bauer, M.; Davies, F.E.; Rosenthal, A.; Wang, H.; Qu, P.; Hoering, A.; et al. Identification of Novel Mutational Drivers Reveals Oncogene Dependencies in Multiple Myeloma. *Blood* **2018**, *132*, 587–597. [[CrossRef](#)]
36. Sudha, P.; Ahsan, A.; Ashby, C.; Kausar, T.; Khera, A.; Kazeroun, M.H.; Hsu, C.-C.; Wang, L.; Fitzsimons, E.; Salminen, O.; et al. Myeloma Genome Project Panel Is a Comprehensive Targeted Genomics Panel for Molecular Profiling of Patients with Multiple Myeloma. *Clin. Cancer Res.* **2022**, *28*, OF1–OF11. [[CrossRef](#)] [[PubMed](#)]
37. Kim, M.; Jeon, K.; Hutt, K.; Zlotnicki, A.M.; Kim, H.J.; Lee, J.; Kim, H.S.; Kang, H.J.; Lee, Y.K. Immunoglobulin gene rearrangement in Koreans with multiple myeloma: Clonality assessment and repertoire analysis using next-generation sequencing. *PLoS ONE* **2021**, *16*, e0253541. [[CrossRef](#)]
38. Medina, A.; Jiménez, C.; Sarasquete, M.E.; González, M.; Chillón, M.C.; Balanzategui, A.; Prieto-Conde, I.; García-Álvarez, M.; Puig, N.; González-Calle, V.; et al. Molecular profiling of immunoglobulin heavy-chain gene rearrangements unveils new potential prognostic markers for multiple myeloma patients. *Blood Cancer J.* **2020**, *10*, 14. [[CrossRef](#)] [[PubMed](#)]
39. Ferrero, S.; Capello, D.; Svaldi, M.; Boi, M.; Gatti, D.; Drandi, D.; Rossi, D.; Barbiero, S.; Mantoan, B.; Mantella, E.; et al. Multiple myeloma shows no intra-disease clustering of immunoglobulin heavy chain genes. *Haematologica* **2012**, *97*, 849. [[CrossRef](#)]
40. Hadzidimitriou, A.; Stamatopoulos, K.; Belessi, C.; Lalayianni, C.; Stavroyianni, N.; Smilevska, T.; Hatzi, K.; Laoutaris, N.; Anagnostopoulos, A.; Kollia, P.; et al. Immunoglobulin genes in multiple myeloma: Expressed and non-expressed repertoires, heavy and light chain pairings and somatic mutation patterns in a series of 101 cases. *Haematologica* **2006**, *97*, 781–787.